Received April 16, 2020, accepted May 15, 2020, date of publication May 26, 2020, date of current version June 23, 2020.

Digital Object Identifier 10.1109/ACCESS.2020.2997789

Novel Sector Two-Dimensional Crest Factor Reduction Techniques for Performance Improvement in Dual-Band System

CHEN CHANGWEI[1,2], KAIYU QIN[1,2], (Member, IEEE), HAIBO MEI[1], BO TANG[1], AND YONG CAO[1]

[1]School of Aeronautics and Astronautics, University of Electronic Science and Technology of China, Chengdu 611731, China
[2]Aircraft Swarm Intelligent Sensing and Cooperative Control Key Laboratory of Sichuan Province, Chengdu 611731, China

Corresponding author: Bo Tang (tangbocd@uestc.edu.cn)

ABSTRACT Currently, peak-to-average power ratio (PAPR) degrades the performance of the wireless system and has been widely studied in the orthogonal frequency division multiplexing (OFDM) systems. However, there is less work concerning about this issue in the dual-band signal wireless communication system, which still hinders the wide applications of the system. This paper aims to develop a new two-dimensional sector crest factor reduction (2D-SCFR) method to solve this problem in the dual-band signal system by reducing a certain amount of dual-band signal amplitude. In practice, we formulate a combined PAPR of the dual-band signals with the independent Gaussian distribution to evaluate the PAPR value of the dual-band signals. Further, as to the peak detection process, this proposed method introduces a continuous piecewise function, which determines the reduction amount based on signal amplitude to avoid over-reduction. To evaluate the performance of the proposed clipping technique, crest factor reduction (CFR) algorithms are applied as the benchmark solution with different dual-band input signal combinations. The numerical results show that the proposed method significantly improves the signal quality of error vector magnitude (EVM), as compared to other CFR algorithms.

INDEX TERMS Dual-band, PAPR, 2D-CFR, power amplifier.

I. INTRODUCTION

With the rapid development of mobile communication, a plurality of modern communication systems with different coexisting carrier frequencies have emerged to improve the services and increase the data rates. In order to increase the efficiency of the base station, it is necessary to integrate different communication systems with different carrier frequencies into the same device. Recently, various technologies on dual-band transmitters, including dual-band filters [1], [2], dual-band power amplifiers [3], [4], and dual-band antennas [5], have been proposed to support concurrent dual-/multi-band communication.

Modern mobile communications, such as wideband code division multiple access (WCDMA) and orthogonal frequency division multiplexing(OFDM), have features of complex modulation, high spectral efficiency and broad bandwidth. Those systems are also affected by the high peak-to-average power ratio (PAPR) issue. Those existing complex modulations need the power amplifier operating in the back-off region from the saturation point to meet the high linearity requirements, therefore resulting in lower power efficiency. A practical problem that hinders a multi-standard system from being integrated into concurrent dual-/multi-band systems is that the dual-band signal significantly increases the peak-to-average power ratio (PAPR) and worsens the nonlinearity and efficiency of the power amplifier in contrast with the single-band signal.

As to the problem, crest factor reduction (CFR) [6] is an effective method to reduce the power amplifier back-off and improve its efficiency with limited signal quality degradation. In practice, several CFR techniques applied in single-band signals can be divided into two categories: signal distortion techniques and signal scrambling techniques. The signal distortion techniques, such as signal clipping [6], peak windowing [7] and nonlinear companding transform (NCT) [8], reduce the PAPR of the input signal by distorting the signal and have been widely used due to the simplicity

The associate editor coordinating the review of this manuscript and approving it for publication was Vittorio Camarchia.

and adaptability. The signal scrambling techniques [9]–[11], such as block coding, partial transmit sequence (PTS), selected mapping [12], tone reservation [13], could achieve a better CFR amount without significant signal deterioration. However, the signal scrambling techniques require the receiver to process the signal accordingly [14]. Due to the different communication standards/modulation schemes applied in each band, it is difficult to apply the signal scrambling techniques to dual-band signals because of the incompatibility issue.

The signal distortion-based clipping technology is widely applied by CFR for single-/multi-band signals. The conventional one-dimensional CFR (1D-CFR) [15], [16] compares each band with the threshold value. Each band signal is processed by clipping and filtering when its amplitude exceeds the threshold value. Since the combining effect of the amplitudes of dual-band signals is not taken into account, there will be over-reduction or under-reduction issues. The over-reduction will deteriorate the signal quality unnecessarily, and the under-reduction issue will deteriorate the output signal PAPR reduction and decrease the efficiency.

Compared to the single-band signal CFR, the combining effect of independent dual-band signals needs to be taken into account to evaluate the peak value and adjust the clipping amount carefully between two bands, so as to balance the reduction amount and the signal quality. To improve the efficiency of dual-/multi-band transmitters, a two-dimensional CFR (2D-CFR) algorithm has been studied simultaneously with the development of the two-dimensional digital predistortion technology [17]–[19].

In [16], [20]–[24], 2D-CFR is studied as a PAPR reduction technology for wireless communication on dual-band transmitters. The literature [16] firstly considers the combination of dual-band signals in the clipping method. In [16], the instantaneous power sum of two bands with a predefined threshold is used to evaluate the peak value, and determine the reduction amount of dual-band signal. The 2D-CFR method jointly clips the dual-band signals with the same proportion, which corrects the defects of 1D-CFR that fails to consider the combining effect of a dual-band system and significantly improves the performance of the CFR method on dual-band signals. The 2 component carriers-CFR (2CC-CFR) technology in [22] extends its application scope to the scenarios of unequal power levels, and considers different requirements on error vector magnitude (EVM) and arbitrary number of carriers. The two-dimensional modified CFR (2D-MCFR) proposed in [24] uses the difference of signal instantaneous amplitude between the two bands to determine the reduction amount of the two bands. However, the 2D-MCFR algorithm brings in defects of signal discontinuity, leading to deterioration of signal quality, which will be analyzed in detail in Section III.

Effective 2D-CFR requires calculation of the combining PAPR correctly. However, there is no literature to theoretically analyze and calculate the combining PAPR of concurrent dual-band signals. Instead, different peak evaluation methods have been studied. For example, the literatures [16], [21] use the power sum of the dual-band signals to evaluate the peak value and determine the reduction amount, while the literature [24] uses the signal amplitude sum of the dual-band signal to evaluate the peak value and determine the reduction amount. In this paper, a theoretical formula is derived on the PAPR of the dual-band signal. At the same time, in order to further improve the performance of the dual-band clipping method, a 2D sector CFR (2D-SCFR) method is proposed to determine the CFR amount with a continuous piecewise function based on the amplitude of the dual-band signals. This method takes advantage of the appropriate continuous reduction amount and gets a better distortion performance.

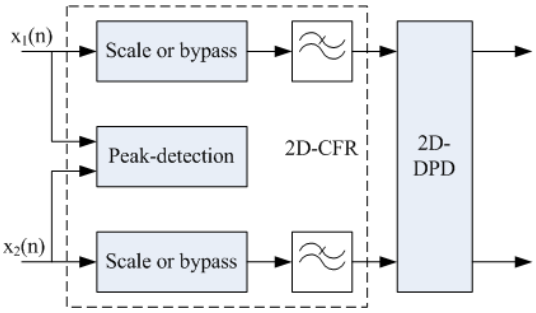

FIGURE 1. Concurrent dual-band transmitter model with 2D-CFR module.

In the end of this paper, two dual-band communication signals with different PAPR values are processed by the proposed 2D-SCFR method and the conventional method. The simulation results prove that the proposed 2D-SCFR gives a better performance on PAPR reduction and EVM of signal quality by correcting the defects including over-reduction, under-reduction and signal discontinuity. The resulted PAPR and the signal quality are both improved as compared to the conventional CFR methods.

The following part of this paper is as follows. Section II introduces the existing methods. The explicit formula describing the PAPR of the dual-band signal and the proposed 2D-SCFR algorithm are deduced in Section III. Section IV gives simulation results of different 2D-CFR methods. The conclusions are drawn in Section V.

II. EXISTING CFR METHODS FOR DUAL-BAND SIGNALS

A concurrent dual-band wireless communication transmitter implemented with 2D-CFR and two-dimensional digital predistortion (2D-DPD) algorithms is shown in Fig. 1. CFR is used to reduce the PAPR value of the input signal and improve the efficiency of the power amplifier.

In order to represent different clipping methods, such as 1D-CFR, 2D-CFR, 2D-MCFR, etc., the dual-band signal is represented as a 2D vector pair $(x_1(n), x_2(n))$, and 2D power/amplitude reduction direction and position for each pair of sampling point vectors are drawn with respect to different CFR algorithms.

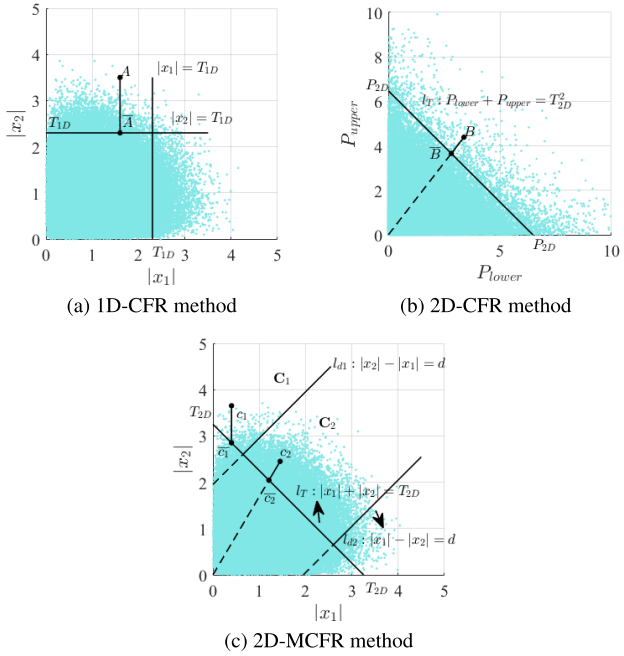

(a) 1D-CFR method (b) 2D-CFR method

(c) 2D-MCFR method

FIGURE 2. The clipping process of existing CFR methods.

A. 1D-CFR ALGORITHM

The 1D-CFR algorithm [16] is widely used in various communication systems. The 1D-CFR algorithm is simply used to clip each band signal without considering the combination of the dual-band signals. The two bands signals are compared with the threshold respectively, and are clipped.

Fig. 2(a) shows the clipping process of the 1D-CFR method, where the line $|x_1| = T_{1D}$ and the line $|x_2| = T_{1D}$ represent the CFR thresholds. According to the 1D-CFR clipping algorithm, point A will be clipped to point $\bar{A}$ in the direction of the parallel coordinate axis. Obviously, the amount of clipping is under-reduction.

B. 2D-CFR ALGORITHM

In 2D-CFR algorithm [21], $P_{sum}(n)$ in (1) is introduced in the peak detector to represent the sum of the dual-band signal power.

$$P_{sum}(n) = |x_1(n)|^2 + |x_2(n)|^2 \tag{1}$$

Then $P_{sum}(n)$ is compared with threshold P_{2D}, and 2D-CFR method is described as

$$(\overline{x_1}(n), \overline{x_2}(n)) = \begin{cases} (x_1(n), x_2(n)), & P_{sum}(n) \geqslant P_{2D} \\ \sqrt{\dfrac{P_{2D}}{P_{sum}(n)}}(x_1(n), & x_2(n)) \\ & P_{sum}(n) < P_{2D} \end{cases} \tag{2}$$

where $\overline{x_1}(n)$ and $\overline{x_2}(n)$ are the clipped signals.

Fig.2 (b) shows the 2D-CFR method which takes into account the combining effect of dual-band signals. The line $L_T : |P_{lower}| + |P_{upper}| = P_{sum}$ is the clipping threshold. According to the 2D-CFR algorithm in (2), the sampling point B is clipped to point $\overline{B}$ which is the intersection of the line OB and the threshold line L_T. The obvious defect of this algorithm is that, if the power sum of the two bands is higher than the threshold P_{2D}, the instantaneous amplitude value of one band is still clipped with the same proportion as the other band even if it is low. This will lead to unnecessary over-reduction, thereby deteriorating the signal quality.

At the same time, the reduction amount is insufficient with P_{sum} as the threshold instead of the amplitude sum. This results in the peak value not being effectively clipped. The 2D-PDR algorithm [21] optimizes the amount of dual-band clipping according to the maximum available power distribution (MAPD) of the power amplifier.

C. 2D-MCFR ALGORITHM

To ameliorate the over-reduction issue of 2D-CFR, the 2D-MCFR method [24] takes d as the instantaneous amplitude difference parameter to determine the reduction amount of the two bands during peak detection. When the signal amplitude difference is higher than d, the weaker signal will not be clipped to avoid over-reduction of the weaker signal. The algorithm could be described as follows:

If $|x_1(n)| + |x_2(n)| < T_{2D}$, each band signal will remain unchanged which is formulated as follows:

$$\begin{cases} |\overline{x_1}(n)| = |x_1(n)| \\ |\overline{x_2}(n)| = |x_2(n)| \end{cases} \tag{3}$$

If $|x_1(n)| + |x_2(n)| > T_{2D}$, $|(|x_1(n)| - |x_2(n)|)| > d$, and $|x_2(n)| > |x_1(n)|$, the clipping method can be expressed as:

$$\begin{cases} |\overline{x_1}(n|) = |x_1(n)| \\ |\overline{x_2}(n)| = T_{2D} - |x_1(n)| \end{cases} \tag{4}$$

where only the stronger signal $x_2(n)$ is clipped, the weaker signal $x_1(n)$ remains unchanged and vice versa, which is shown in (5). When $|x_1(n)| + |x_2(n)| > T_{2D}$, and $|(|x_1(n)| - |x_2(n)|)| > d$, $|x_1(n)| > |x_2(n)|$, the clipped signal can be expressed as:

$$\begin{cases} |\overline{x_1}(n)| = T_{2D} - |x_2(n)| \\ |\overline{x_2}(n)| = |x_2(n)| \end{cases} \tag{5}$$

Similar to 2D-CFR, if $|x_1(n)| + |x_2(n)| > T_{2D}$, and $|(|x_1(n)| - |x_2(n)|)| < d$, $|x_1(n)|$ and $|x_2(n)|$ are clipped with the same proportion. Then the clipped signal can be expressed as:

$$\begin{cases} |\overline{x_1}(n)| = \dfrac{T_{2D}}{|x_1(n)| + |x_2(n)|}|x_1(n)| \\ |\overline{x_2}(n)| = \dfrac{T_{2D}}{|x_1(n)| + |x_2(n)|}|x_2(n)| \end{cases} \tag{6}$$

Fig. 2(c) shows the 2D-MCFR method which uses instantaneous amplitude difference of a dual-band signal to correct the over-reduction defect of a smaller signal. Points c_1 and c_2 are the sampling points defined in region C_1 and C_2. According to the 2D-MCFR algorithm in (4) and (6), the sampling points c_1 and c_2 are clipped to points $\overline{c_1}$ and $\overline{c_2}$ respectively.

III. THE PAPR FORMULATION DERIVATION AND THE PROPOSED CFR SCHEME

A. DERIVATION OF THE PAPR FORMULATION OF DUAL-BAND SIGNALS

In wireless communication systems, such as WCDMA and long term evolution (LTE), quadrature modulation signals I and Q accurately follow the Gaussian-distribution with zero mean, and their amplitudes follow a Rayleigh distribution [25]. Since the dual-band signals are generated from different signal sources, it can be believed that the signals of two bands are independent and uncorrelated.

Accordingly, the PAPR of a single-band or multi-band signal $x(n)$ can be defined as the ratio of the maximum power to the average power as follows:

$$PAPR[x(n)] = 10log_{10}\frac{max[|x(n)|^2]}{E[|x(n)|^2]} \tag{7}$$

where $E[|x(n)|^2]$ is the mean power of the signal, and $max[\cdot]$ is the maximum value of the square of signal amplitude $|x(n)|$.

In a dual-band transmitter, the complex baseband signals of the lower band and the upper band are defined as $x_1(n)$ and $x_2(n)$, respectively, as follows:

$$\begin{cases} x_1(n) = x_{1i}(n) + j * x_{1q}(n) \\ x_2(n) = x_{2i}(n) + j * x_{2q}(n) \end{cases} \tag{8}$$

The baseband complex signals are modulated into each of their lower and upper bands by modulators and then combined. Without loss of generality, the discrete-time baseband can be expressed as (9), which is equivalent to the dual-band signal after combination.

$$x(n) = x_1(n)e^{-j\omega nT_s} + x_2(n)e^{j\omega nT_s} \tag{9}$$

where $\omega = \Delta\omega/2$, $\Delta\omega$ is the difference between the center frequencies of the lower and upper bands, and Ts is the sampling period of the baseband signal.

$|x(n)|^2$ in the (7) can be calculated as follows:

$$\begin{aligned} |x(n)|^2 &= x(n)x^*(n) \\ &= (x_1(n)e^{-j\omega nT_s} + x_2(n)e^{j\omega nT_s}) \\ &\quad \times (x_1^*(n)e^{j\omega nT_s} + x_2^*(n)e^{-j\omega nT_s}) \\ &= |x_1(n)|^2 + |x_2(n)|^2 \\ &\quad + x_1(n)x_2^*(n)e^{-j2\omega nT_s} + x_2(n)x_1^*(n)e^{j2\omega nT_s} \end{aligned} \tag{10}$$

As mentioned earlier, $x_1(n)$ and $x_2(n)$ are independent and follow a zero-mean Gaussian distribution, which can be denoted as

$$\begin{cases} E[x_1(n)x_2^*(n)] = E[x_1(n)]E[x_2^*(n)] = 0 \\ E[x_2(n)x_1^*(n)] = E[x_2(n)]E[x_1^*(n)] = 0 \end{cases} \tag{11}$$

Therefore, the expected value of $|x(n)|^2$ from the expression (10) can be obtained as

$$E[|x(n)|^2] = E[|x_1(n)|^2] + E[|x_2(n)|^2] \tag{12}$$

To calculate $max[|x(n)|^2]$, (8) is substituted into (10), and $|x(n)|^2$ could be deduced as follows:

$$\begin{aligned} |x(n)|^2 &= |x_1(n)|^2 + |x_2(n)|^2 + 2(x_{1i}x_{2i} + x_{1q}x_{2q}) \\ &\quad \times cos(\Delta\omega nT_s) + 2(x_{1q}x_{2i} - x_{1i}x_{2q})sin(\Delta\omega nT_s) \\ &= |x_1(n)|^2 + |x_2(n)|^2 + 2Acos(\Delta\omega nT_s + \theta) \\ &\leqslant |x_1(n)|^2 + |x_2(n)|^2 + 2A \end{aligned} \tag{13}$$

where $A = \sqrt{(x_{1i}x_{2i} + x_{1q}x_{2q})^2 + (x_{1q}x_{2i} - x_{1i}x_{2q})^2}$, $\theta = arctan(x_{1i}x_{2q} - x_{1q}x_{2i})/(x_{1i}x_{2i} + x_{1q}x_{2q})$. It could be easily found that when $\Delta\omega nT_s + \theta = (k + 1/2)\pi$ or $t = nT_s = (k+1/2)\pi/\Delta\omega$, the function $max[|x(n)|^2]$ reaches its highest point.

It could be deduced easily from (8) that

$$(|x_1(n)| + |x_2(n)|)^2 = |x_1(n)|^2 + |x_2(n)|^2 + 2A \tag{14}$$

Comparing (13) with (14), we can get $|x(n)|^2 \leq (|x_1|^2 + |x_2(n)|^2$, which is substituted into (7) together with (12) to obtain the PAPR value of the dual-band signal.

$$PAPR[x(n)] = 10log_{10}\frac{max[(|x_1(n)| + |x_2(n)|)^2]}{E[(|x_1(n)| + |x_2(n)|)^2]} \tag{15}$$

This formula shows that the PAPR of the dual-band signal $x(n)$ is the ratio of the square of the amplitude sum of the two single-band signals to the average power of the dual-band signals.

To describe the PAPR value between the single-band signal and the dual-band signal, two kinds of concurrent dual-band signals are considered as follows,

1) The input signals of the lower and upper bands are WCDMA signals and OFDM signals. The WCDMA signals are applied as the lower band, in which a PAPR value of complementary cumulative distribution function (CCDF) for 0.1% is 8.4 dB. The OFDM signals modulated by 4-quadrature amplitude modulation (4-QAM) are applied as the upper band with a PAPR value of 10.2 dB.

The separate PAPR value and the joint PAPR value are shown in Fig. 3(a), where the joint PAPR value is 10.6dB. It can be seen in the figure that the joint PAPR value is higher than both PAPR values of the WCDMA signals and the OFDM signals, since the peak value of the joint dual-band signal is the sum of the two band peak values.

2) The input signals of the lower and upper bands are both OFDM signals. The lower band is modulated by 4QAM with a PAPR value of 10.2 dB. The OFDM signals modulated by 16QAM are applied as the upper band with a PAPR value of 10.2 dB.

The separate PAPR values and the joint PAPR value are shown in Fig. 3(b), which demonstrate the increase of the PAPR value of the joint signal as compared to each band. In Fig. 3(b), the red and green curves are the separate PAPR value curves while the black curve is the joint PAPR value. Compared to single-band signal, dual-band signal has a higher PAPR with the dual-band combining effect as formulated in (15).

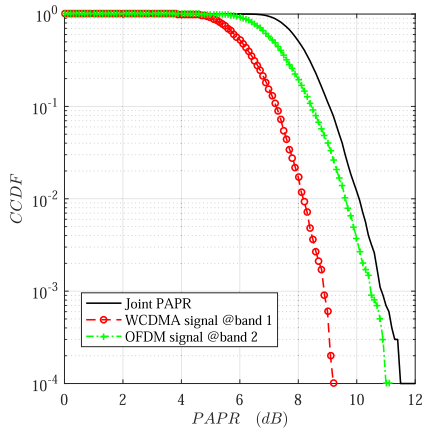

(a)

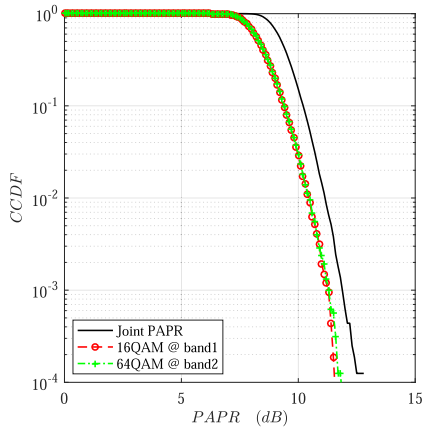

(b)

FIGURE 3. Theoretical CCDF performance of dual-band signals.

It is worth noting that after the joint clipping operation, the independence condition of the dual-band signal is no longer strictly matched, which will bring some errors to the PAPR calculation. Since the WCDMA and OFDM signals are normally distributed, and the amplitude distribution of WCDMA and OFDM modulated signals follows the Rayleigh distribution [25], the probability of large peak clipping is very small, so that the error of the CFR of the PAPR value is ignorable.

B. THE PROPOSED 2D-CFR REDUCTION SCHEME

Different 2D-CFR algorithms use different peak detection methods to determine the reduction amount of the two bands. The peak detection module is the key to reduce the defects of over-reduction and under-reduction, thereby, influencing the performance of the 2D-CFR method. The 2D-MCFR method avoids over-reduction, but it results in a new problem of signal discontinuity.

In Fig. 4, point c is the sampling point defined as the amplitude difference d between the two signal bands, i.e. $|x_1(c)| - |x_2(c)| = d$. It can be seen from the figure

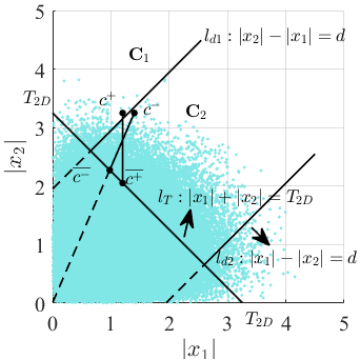

FIGURE 4. Concurrent dual-band transmitter model with 2D-CFR module.

that the signal discontinuity occurs on point c. Point c^+ is a single-sided signal from the right-hand direction $|x_2(c)| - |x_1(c)| \to d^+$. According to (4), point c^+ will be clipped to point $\overline{c^+}$, which is $(|x_1(c)|, T_{2D} - |x_1(c)|)$.

Point c^- is a single-sided signal from the left-hand direction $|x_2(c)| - |x_1(c)| \to d^-$. According to (6), point c^- will be clipped to point $\overline{c^-}$, which is $(\frac{T}{|x_1(c)|+|x_2(c)|}|x_1(c)|, \frac{T}{|x_1(c)|+|x_2(c)|}|x_2(c)|)$. Therefore, since the two single-sided limits are unequal, the clipped signal is not continuous while the vector pair $(x_1(n), x_2(n))$ approaches the line $|x_1(n)| - |x_2(n)| = d$, as shown in (16).

$$\begin{cases} |\overline{x_1}(c^+)| \neq |\overline{x_1}(c^-)| \\ |\overline{x_2}(c^+)| \neq |\overline{x_2}(c^-)| \end{cases} \tag{16}$$

The single-sided clipped signals $\overline{c^+}$ and $\overline{c^-}$ are much different while point c is in the vicinity of line of l_{d_1} or l_{d_2}. As a result, the clipped signal amplitude is discontinuous, serious peak regeneration and distortion will be generated and the signal quality will be deteriorated.

In order to further optimize the 2D-CFR performance, the clipping amount is appropriately reduced and the signal continuity in the clipping process is taken into account. Therefore, a 2D-SCFR algorithm with a continuous piecewise function is proposed. The process is detailed as follows.

Given that the threshold of the dual-band signal is T_{2D}, when $|x_1(n)| + |x_2(n)| < T_{2D}$, the signals remain unchanged, which is shown as follows:

$$\begin{cases} |\overline{x_1}(n)| = |x_1(n)| \\ |\overline{x_2}(n)| = |x_2(n)| \end{cases} \tag{17}$$

where $\overline{x_1}(n)$ and $\overline{x_2}(n)$ are the clipped signals.

When the instantaneous amplitude of the dual-band signal exceeds the predefined threshold $|x_1(n)| + |x_2(n)| > T_{2D}$, the joint clipping process has to be performed. In the conventional 2D-CFR method, even though the instantaneous value of a signal is low, it will be clipped with the same proportion as the higher one. This leads to an unnecessary over-reduction. To avoid over-reduction, the weaker signal $x_1(n)$ remains unchanged during the clipping process due to

its negligible contribution to the nonlinearity of the dual-band signal. Thus, only the strong signal amplitude $|x_2(n)|$ is clipped. To guarantee that the peak value of the clipped dual-band signal is less than the threshold T_{2D}, i.e. $|x_2(n)| + |x_2(n)| \leq T_{2D}$, only the strong signal amplitude is clipped as $|\overline{x_2}(n)| = T_{2D} - |x_1(n)|$, which is shown in (18).

If $|x_1(n)| + |x_2(n))| > T_{2D}$ and $|x_1(n)| < p$, the algorithm is described as:

$$\begin{cases} |\overline{x_1}(n)| = |x_1(n)| \\ |\overline{x_2}(n)| = T_{2D} - |x_1(n)| \end{cases} \tag{18}$$

where the value of p is determined by the signal mean and threshold of the two bands, and $p < min(mean(|x_1(n)|), mean(|x_2(n)|), T_{2D}/2)$.

Similarly, if $|x_1(n)| + |x_2(n)| > T_{2D}$ and $|x_2(n)| < p$, only $x_1(n)$ has to be clipped, which is described as:

$$\begin{cases} |\overline{x_1}(n)| = T_{2D} - |x_2(n)| \\ |\overline{x_2}(n)| = |x_2(n)| \end{cases} \tag{19}$$

When $|x_1(n)| + |x_2(n)| > T_{2D}$ and the amplitudes of the dual-band signals both exceed the limit p, i.e. $|x_{1,2}(n)| > p$, the dual-band signal is clipped with the same proportion. In order to ensure continuity of the clipped signal and reduce unnecessary distortion in the clipping process, we move the initial coordinate origin point to point (p, p), and the coordinates of the pair of the vector points in the new coordinate system are (g_1, g_2).

$$\begin{cases} g_1(n) = |x_1(n)| - p \\ g_2(n) = |x_2(n)| - p \end{cases} \tag{20}$$

The clipping with the same proportion is performed in the new coordinate system. The threshold in the new coordinate system is $T_{2D} - 2p$ and the scale is $\dfrac{T_{2D} - 2p}{g_1(n) + g_2(n)}$. The clipping process is described as

$$\begin{cases} \overline{g_1}(n) = \dfrac{T_{2D} - 2p}{g_1(n) + g_2(n)} g_1(n) \\ \overline{g_2}(n) = \dfrac{T_{2D} - 2p}{g_1(n) + g_2(n)} g_2(n) \end{cases} \tag{21}$$

Finally, the clipping process is converted to the original coordinate system. Substituting (21) into (20), the resultant dual-band clipped signal is obtained as

$$\begin{cases} |\overline{x_1}(n)| = \dfrac{(T_{2D} - 2p)(|x_1(n)| - p)}{|x_1(n)| + |x_2(n)| - 2p} + p \\ |\overline{x_2}(n)| = \dfrac{(T_{2D} - 2p)(|x_2(n)| - p)}{|x_1(n)| + |x_2(n)| - 2p} + p \end{cases} \tag{22}$$

The p value greatly affects the final EVM, so the EVM may be seen as a function of p in the proposed scheme. It is important to choose the optimized value of p parameter to minimize the EVM value. Let $q = min(mean(|x_1|), mean(|x_2|), T_{2D}/2)$. Therefore, minimizing $EVM(p)$ can be described by the following optimization problem.

$$\begin{aligned} &Minimize \quad EVM(p) \\ &subject\ to \quad 0 < p < q \end{aligned} \tag{23}$$

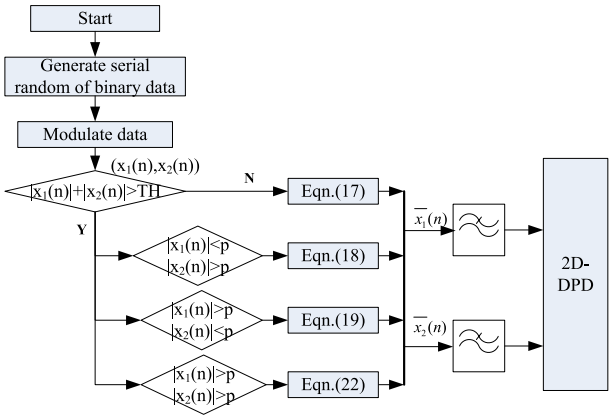

FIGURE 5. The flow chart of the proposed peak clipping method.

The optimization problem can be solved by the convex optimization method to determine the optimized p value.

The flow chart of the proposed clipping method is shown in Fig. 5. The algorithm includes signal generation, signal modulation, peak detection, peak clipping and filtering, where the clipping step is a switch process. The amount of clipping is determined by the nonlinear contribution of the amplitude of each band signal.

C. THE PERFORMANCE ANALYSIS OF 2D-CFR IN DUAL-BAND SIGNAL

1) SIGNAL CONTINUITY OF THE PROPOSED SCHEME

Fig. 6 illustrates the proposed 2D-CFR method by showing the vectors of an unclipped signal and the resultant clipped sample. The threshold line $|x_1(n)|+|x_2(n)| = T_{2D}$ determines whether to clip the peak signals. The lines $l_{d1} : |x_1| = p$ and $l_{d2} : |x_2| = p$ represent the sector level of the signal.

As shown in Fig. 6, points d_1 and d_2 are the sampling points defined in regions D_1 and D_2. For point d on the sector level line, i.e. $|x_1(d)| = p$, according to (18), point d^- will be clipped to point $\overline{d^-}$,

$$\begin{cases} |\overline{x_1}(d^-)| = \lim\limits_{|x_1(d)| \to p^-} |x_1(d)| = p \\ |\overline{x_2}(d^-)| = \lim\limits_{|x_1(d)| \to p^-} |x_2(d)| \\ \qquad\qquad = T_{2D} - p \end{cases} \tag{24}$$

where point $\overline{d^-}$ is a single-sided clipped signal from the right-hand direction $|x_1(d^-)| \to p^-$. Similarly, according to (20), point d^+ will be clipped to point $\overline{d^+}$.

$$\begin{cases} |\overline{x_1}(d^+)| = \lim\limits_{|x_1(d)| \to p^+} |\overline{x_1}(d)| = p \\ |\overline{x_2}(d^+)| = \lim\limits_{|x_1(d)| \to p^+} |\overline{x_2}(d)| \\ \qquad\qquad = T_{2D} - p \end{cases} \tag{25}$$

where point $\overline{d^+}$ is a single-sided clipped signal from the left-hand direction $|x_1| \to p^+$. Therefore, the two single-sided limits are equal, and the clipped signal is continuous as the

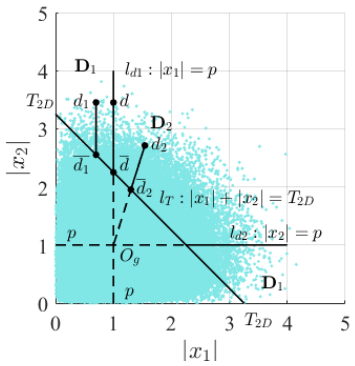

FIGURE 6. The clipping process of the proposed 2D-SCFR methods.

vector pair (x_1, x_2) approaches the line $x_1 = p$, which is shown as follows.

$$\begin{cases} |\overline{x_1}(d^+)| = |\overline{x_1}(d^-)| \\ |\overline{x_2}(d^+)| = |\overline{x_2}(d^-)| \end{cases} \tag{26}$$

It can be seen from Fig. 6 that the proposed clipping algorithm keeps the continuity of the signal after the signal is clipped, and avoids over-reduction and under-reduction.

2) CCDF AND EVM PERFORMANCE ANALYSIS OF THE PROPOSED SCHEME

In this section, in order to evaluate the performance of the proposed method, CCDF and EVM are used to work as the criteria to evaluate the performance of the proposed method. The CFR algorithm can suppress the PAPR value of the signals, and improve the efficiency of a power amplifier. The amount of PAPR reduced by CFR can be represented by CCDF [25], which is expressed as follows:

$$CCDF = P_r(PAPR > \gamma) \tag{27}$$

where γ is the expected threshold, and P_r is the proability of {.}.

Afterwards, because the clipping algorithm will bring distortion to the signal to some extent, the out-of-band distortion of the algorithm indicates that the spectrum leakage can be suppressed by the filter. To evaluate this point, the in-band distortion of the output signal will be characterized by EVM to evaluate the influence of different clipping algorithms on signal distortion. EVM is a criterion that can be comprehensively measured to show the signal amplitude error and phase error, and can reflect the error before and after clipping. EVM can be defined as

$$EVM = \frac{\|x - \bar{x}\|_2}{\|x\|_2} \tag{28}$$

IV. SIMULATION

In this section, the performance of the proposed 2D-SCFR is simulated and compared to traditional clipping methods considering two different scenarios. Those scenarios under consideration include diverse PAPR values and similar PAPR values between dual-band signals to evaluate the generality of the proposed method.

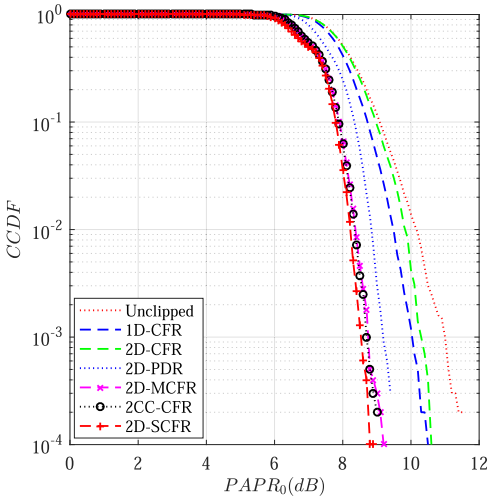

FIGURE 7. PAPR performance evaluation of the 2D clipping methods.

A. DIVERSE PAPR VALUE SCENARIO

In this subsection, the signals used in the simulation are WCDMA (bandwidth: 5MHz) signals and OFDM signals (bandwidth: 5MHz). WCDMA is a third-generation (3G) wideband spread spectrum standard that employs the direct-sequence code division multiple access (DS-CDMA) channel as the access method. Firstly, WCDMA and OFDM bit sources are generated in this simulation, WCDMA signals are modulated and mapped by the 16-quadrature amplitude modulation (16QAM) scheme, and OFDM signals are modulated by the 4QAM.

The output signal has an oversampling rate of $L = 4$. The OFDM signal divides the wideband into N parallel orthogonal subcarriers. In this paper, the subcarrier N is set to 64. After the source signals are generated, the OVSF code is used for spreading spectrum. In this paper, the OVSF length is set to 64, and then the signal is modulated with 16QAM and filtered with a root raised cosine filter. To facilitate the calculation of the simulation, it is assumed that the two signals have been synchronized.

1) PAPR REDUCTION EVALUATION

In this section, the proposed 2D-CFR method and the conventional method are evaluated with $\gamma = 2$ and the two algorithms are compared with different PAPR values. The CCDF curves of the dual-band signal are shown in Fig. 7. Based on the results, the CCDF values of 1D-CFR and 2D-CFR methods are the worst as the dual-band signal is not appropriately clipped. The 2D-PDR method uses a two-dimensional power distribution reshaping (2D-PDR) technique and gets better clipping reduction than 2D-CFR. The expected thresholds of the 2D-MCFR, the 2CC-CFR and the 2D-SCFR method are the same, and the PAPR of the proposed 2D-SCFR method is better than that of the 2D-MCFR algorithm. The 2D-MCFR algorithm causes signal discontinuity and leads to more peak regrowth [26] after filtering.

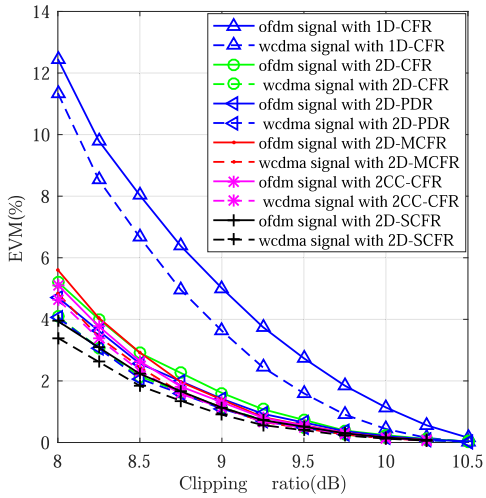

FIGURE 8. Comparison of EVM distortion performance between different clipping methods.

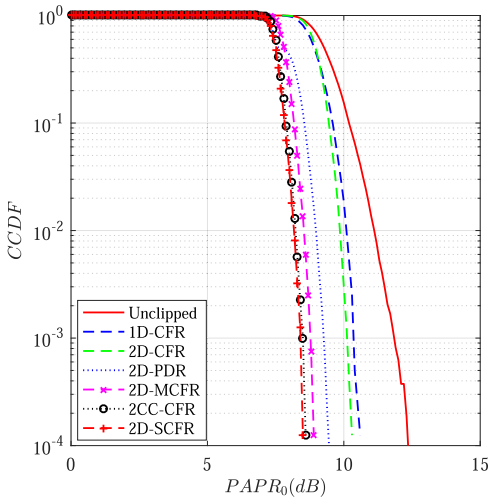

FIGURE 9. PAPR performance evaluation of the 2D clipping methods.

2) EVM ASSESSMENT

In this section, we compare performance of the distortion caused by different clipping algorithms under the same PAPR values. To do so, several EVM and PAPR values are obtained by setting different clipping ratios. The relationships between EVM and PAPR in different clipping methods are obtained by general cubic interpolation, as shown in Fig. 8. The dotted line in Fig.8 represents the EVM value of the lower-band WCDMA signal, and the solid line represents the EVM value of the upper-band OFDM signal. The x-axis represents the resultant target threshold. It can be seen from the figure that the EVM value of the crest reduction method is optimal under the same PAPR while both the reduction amount and signal quality are taken into account.

B. SIMILAR PAPR SCENARIO

In a similar PAPR scenario, the dual-band signal is generated by combining the lower-band OFDM (bandwidth: 20MHz) signal with the upper-band OFDM signal (bandwidth: 20MHz). The step is the same as that in the other PAPR scenario. The OFDM signal of a lower band is modulated and mapped via a 4QAM scheme, and the OFDM signal of an upper band is modulated and mapped via a 16QAM scheme. The output signal has an oversampling rate of $L = 4$. The OFDM signal is divided into 256 parallel orthogonal subcarriers.

1) PAPR ASSESSMENT

Fig. 9 shows the CCDF curves of the dual-band signal with $\gamma = 2$. It could be seen that the peak regrowth is worse as the original signal PAPR increases with the same clipping ratio. The proposed sector clipping is similar to the 2CC-CFR and is marginally better than the 2D-MCFR.

2) EVM ASSESSMENT

Similar to the other PAPR scenario, different methods are compared with respect to EVM. The EVM performance

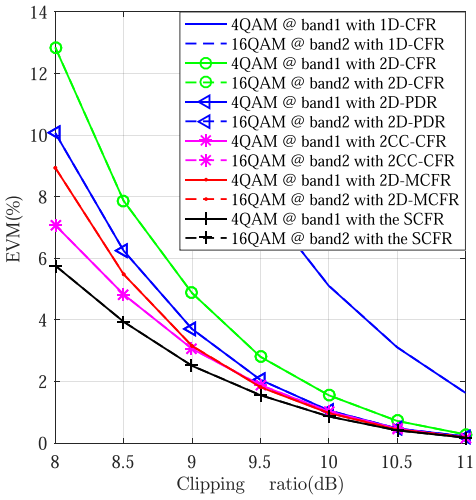

FIGURE 10. Comparison of EVM distortion performance between different clipping methods.

is shown in Fig. 10. We can see that the EVM curves of dual-band signals almost coincide. The performance of the 2D-MCFR method is worse than 2CC-CFR because of its worse discontinuity at the higher PAPR value. The simulation results show that the proposed clipping method gives a better performance on distortion than other clipping methods.

V. CONCLUSIONS

In this paper, a new 2D-SCFR algorithm is proposed for concurrent dual-band communication transmitters to decrease PAPR. The proposed 2D-SCFR algorithm reduces the over-reduction and under-reduction problems in the clipping process while taking into account the signal continuity. After the dual-band signals are clipped and simulated, the proposed method and the traditional method are compared, and the performance of the 2D-CFR algorithm is superior. The simulation results validate that the new 2D-CFR algorithm is superior on the PAPR and EVM performance.

REFERENCES

[1] P. Ma, B. Wei, J. Hong, X. Guo, B. Cao, and L. Jiang, "Coupling matrix compression technique for high-isolation dual-mode dual-band filters," *IEEE Trans. Microw. Theory Techn.*, vol. 66, no. 6, pp. 2814–2821, Jun. 2018, doi: 10.1109/TMTT.2018.2815684.

[2] R. Gomez-Garcia, J.-M. Munoz-Ferreras, W. Feng, and D. Psychogiou, "Balanced symmetrical quasi-reflectionless single- and dual-band bandpass planar filters," *IEEE Microw. Wireless Compon. Lett.*, vol. 28, no. 9, pp. 798–800, Sep. 2018, doi: 10.1109/LMWC.2018.2856400.

[3] T. Cappello, A. Duh, T. W. Barton, and Z. Popovic, "A dual-band dual-output power amplifier for carrier aggregation," *IEEE Trans. Microw. Theory Techn.*, vol. 67, no. 7, pp. 3134–3146, Jul. 2019, doi: 10.1109/TMTT.2019.2895534.

[4] X. Meng, C. Yu, Y. Wu, and Y. Liu, "Design of dual-band high-efficiency power amplifiers based on compact broadband matching networks," *IEEE Microw. Wireless Compon. Lett.*, vol. 28, no. 2, pp. 162–164, Feb. 2018, doi: 10.1109/LMWC.2017.2787058.

[5] R. Chandel, A. K. Gautam, and K. Rambabu, "Tapered fed compact UWB MIMO-diversity antenna with dual band-notched characteristics," *IEEE Trans. Antennas Propag.*, vol. 66, no. 4, pp. 1677–1684, Apr. 2018, doi: 10.1109/TAP.2018.2803134.

[6] L. Yang, X. Lin, X. Ma, and S. Li, "Iterative clipping noise elimination of clipped and filtered SCMA-OFDM system," *IEEE Access*, vol. 6, pp. 54427–54434, 2018, doi: 10.1109/ACCESS.2018.2872723.

[7] S. Cha, M. Park, S. Lee, K.-J. Bang, and D. Hong, "A new PAPR reduction technique for OFDM systems using advanced peak windowing method," *IEEE Trans. Consum. Electron.*, vol. 54, no. 2, pp. 405–410, May 2008, doi: 10.1109/TCE.2008.4560106.

[8] M. Hu, Y. Li, W. Wang, and H. Zhang, "A piecewise linear companding transform for PAPR reduction of OFDM signals with companding distortion mitigation," *IEEE Trans. Broadcast.*, vol. 60, no. 3, pp. 532–539, Sep. 2014, doi: 10.1109/TBC.2014.2339531.

[9] T. Jiang and C. Li, "Simple alternative multisequences for PAPR reduction without side information in SFBC MIMO-OFDM systems," *IEEE Trans. Veh. Technol.*, vol. 61, no. 7, pp. 3311–3315, Sep. 2012, doi: 10.1109/TVT.2012.2201970.

[10] A.-K. Ajami, H. A. Artail, and M. M. Mansour, "PAPR reduction in LTE-advanced carrier aggregation using low-complexity joint interleaving technique," in *Proc. IEEE Wireless Commun. Netw. Conf. (WCNC)*, New Orleans, LA, USA, Mar. 2015, pp. 675–680.

[11] W.-W. Hu, W.-J. Huang, Y.-C. Ciou, and C.-P. Li, "Reduction of PAPR without side information for SFBC MIMO-OFDM systems," *IEEE Trans. Broadcast.*, vol. 65, no. 2, pp. 316–325, Jun. 2019, doi: 10.1109/TBC.2018.2828610.

[12] R. W. Bäuml, R. F. H. Fischer, and J. B. Huber, "Reducing the peak-to-average power ratio of multicarrier modulation by selected mapping," *Electron. Lett.*, vol. 32, no. 22, pp. 2056–2057, Oct. 1996, doi: 10.1049/el:19961384.

[13] J. Hou, J. Ge, and F. Gong, "Tone reservation technique based on peak-windowing residual noise for PAPR reduction in OFDM systems," *IEEE Trans. Veh. Technol.*, vol. 64, no. 11, pp. 5373–5378, Nov. 2015, doi: 10.1109/TVT.2014.2378811.

[14] F. Sandoval, G. Poitau, and F. Gagnon, "Hybrid peak-to-average power ratio reduction techniques: Review and performance comparison," *IEEE Access*, vol. 5, pp. 27145–27161, 2017, doi: 10.1109/ACCESS.2017.2775859.

[15] X. Liu, X. Zhang, J. Xiong, F. Gu, and J. Wei, "An enhanced iterative clipping and filtering method using time-domain kernel matrix for PAPR reduction in OFDM systems," *IEEE Access*, vol. 7, pp. 59466–59476, 2019, doi: 10.1109/ACCESS.2019.2915354.

[16] X. Chen, S. Zhang, and W. Chen, "Two-dimensional crest factor reduction for performance improvement of concurrent dual-band power amplifiers," *Electron. Lett.*, vol. 49, no. 18, pp. 1163–1165, Aug. 2013, doi: 10.1049/el.2013.1650.

[17] C. Yu, C. Fan, X. Meng, J. Li, F. Liu, Y. Liu, and Y. Li, "A square-root-based memory polynomial model for concurrent dual-band digital predistortion," *IEEE Microw. Wireless Compon. Lett.*, vol. 29, no. 2, pp. 152–154, Feb. 2019, doi: 10.1109/LMWC.2018.2886634.

[18] F. Mkadem, A. Islam, and S. Boumaiza, "Multi-band complexity-reduced generalized-memory-polynomial power-amplifier digital predistortion," *IEEE Trans. Microw. Theory Techn.*, vol. 64, no. 6, pp. 1763–1774, Jun. 2016, doi: 10.1109/TMTT.2016.2561279.

[19] H. Enzinger, K. Freiberger, and C. Vogel, "Competitive linearity for envelope tracking: Dual-band crest factor reduction and 2D-vector-switched digital predistortion," *IEEE Microw. Mag.*, vol. 19, no. 1, pp. 69–77, Jan. 2018, doi: 10.1109/MMM.2017.2759618.

[20] W. Chen, X. Chen, and S. Zhang, "Energy-efficient concurrent dual-band transmitter for multistandard wireless communications," in *Proc. AMPC*, Sendai, Japan, 2014, pp. 558–560.

[21] X. Chen, W. Chen, F. Huang, F. M. Ghannouchi, Z. Feng, and Y. Liu, "Systematic crest factor reduction and efficiency enhancement of dual-band power amplifier based transmitters," *IEEE Trans. Broadcast.*, vol. 63, no. 1, pp. 111–122, Mar. 2017, doi: 10.1109/TBC.2016.2619584.

[22] B. Fehri, S. Boumaiza, and E. Sich, "Crest factor reduction of inter-band multi-standard carrier aggregated signals," *IEEE Trans. Microw. Theory Techn.*, vol. 62, no. 12, pp. 3286–3297, Dec. 2014, doi: 10.1109/TMTT.2014.2365788.

[23] B. Fehri and S. Boumaiza, "Joint dual-band crest factor reduction and digital predistortion of power amplifiers driven by inter-band carrier aggregated signals," in *IEEE MTT-S Int. Microw. Symp. Dig.*, Tampa, FL, USA, Jun. 2014, pp. 1–4.

[24] J. Zhao, Y. Liu, C. Yu, J. Yu, and S. Li, "A novel two-dimensional crest factor reduction for performance improvement of RF power amplifiers," *IEEE Microw. Wireless Compon. Lett.*, vol. 25, no. 12, pp. 835–837, Dec. 2015, doi: 10.1109/LMWC.2015.2497162.

[25] K. Anoh, C. Tanriover, B. Adebisi, and M. Hammoudeh, "A new approach to iterative clipping and filtering PAPR reduction scheme for OFDM systems," *IEEE Access*, vol. 6, pp. 17533–17544, 2018, doi: 10.1109/ACCESS.2017.2751620.

[26] L. Yang, K. Song, and Y. M. Siu, "Iterative clipping noise recovery of OFDM signals based on compressed sensing," *IEEE Trans. Broadcast.*, vol. 63, no. 4, pp. 706–713, Dec. 2017, doi: 10.1109/TBC.2017.2669641.

CHEN CHANGWEI received the master's degree in measuring and testing technologies and instruments engineering from the University of Electronic Science and Technology of China. He is currently working with the University of Electronic Science and Technology of China. His current research interests include amplifier linearization, microwave/millimeter wave circuits and systems, electromagnetic theory, and signal processing.

KAIYU QIN (Member, IEEE) received the master's degree in testing technology and instrumentation and the Ph.D. degree in circuits and systems from the University of Electronic Science and Technology of China, in April 1994 and March 1999, respectively. He has been teaching and researching with the University of Electronic Science and Technology of China, since 1994, where he was hired as a Professor, in 2005. He is currently the Dean of the Aircraft Swarm Intelligent Sensing and Cooperative Control Key Laboratory of Sichuan Province. He is a member of the Deep Space Exploration Professional Committee, China Aerospace Society, and the China Aeronautical Society's Near Space Professional Committee. He was awarded the title of Excellent Talent of the New Century by the Ministry of Education, China.

HAIBO MEI received the B.Sc. and M.Sc. degrees from the School of Computer Science and Engineering, University of Electronic Science and Technology of China, in 2005 and 2008, respectively, and the Ph.D. degree from School of Electronic Engineering and Computer Science, Queen Mary University of London (QMUL), U.K., in 2012. He was a Postdoctoral Research Assistant with QMUL and a Senior Research and Development Engineer at Securus Software Ltd., U.K. He is currently a Lecturer with the University of Electronic Science and Technology of China. His research interests include resource efficiency and self-organization of wireless communications, intelligent transportation systems, and mobile cloud computing.

BO TANG received the bachelor's and master's degrees in measuring and testing technologies from the University of Electronics Science and Technology of China, Chengdu, China, in 2005 and 2008, respectively. He is currently a Lecturer with the School of Aeronautics and Astronautics, University of Electronic Science and Technology of China. His research interests include wireless communication, radio frequency and communication testing, and signal processing.

YONG CAO received the bachelor's and master's degrees in measuring and testing technologies from the University of Electronics Science and Technology of China, Chengdu, China, in 2004 and 2007, respectively. He is currently a Lecturer with the School of Aeronautics and Astronautics, University of Electronic Science and Technology of China. His research interests include time domain reflectometry, vector network analyzer, signal integrity analysis and test, high-speed PCB and electronic interconnection system test and fault location, broadband microwave circuit design, and signal processing.